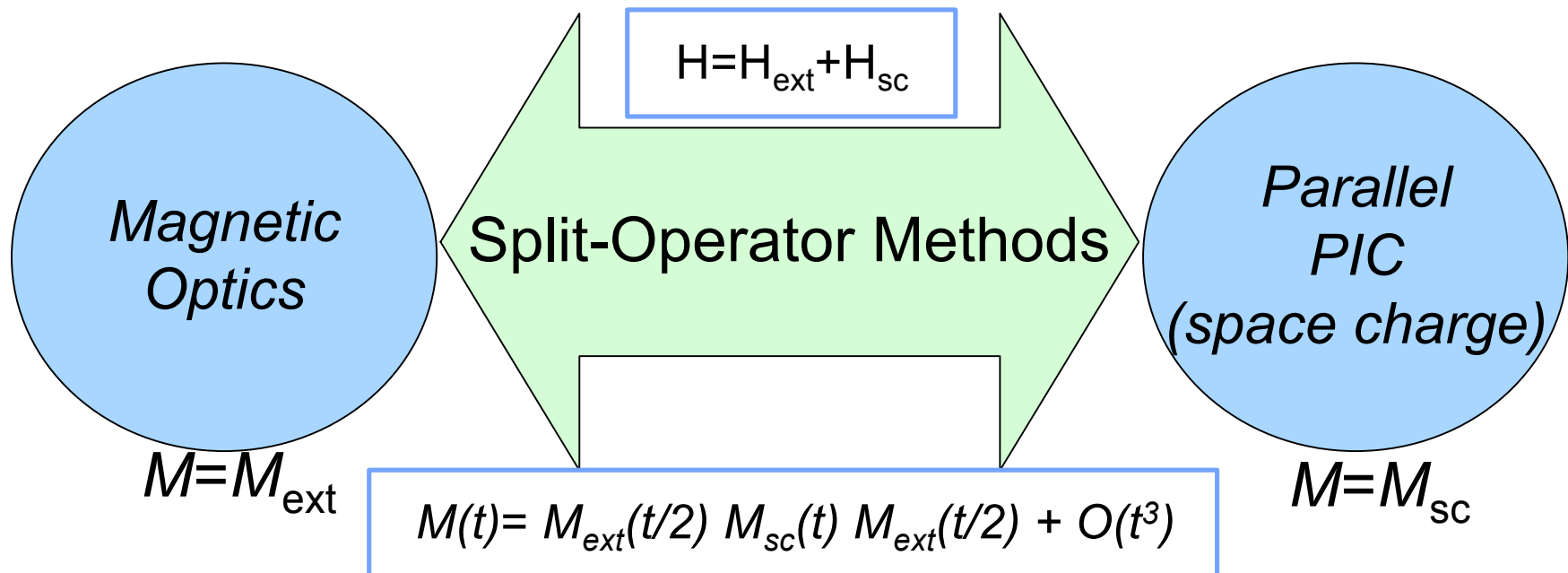


# **Advances in the MaryLie/IMPACT (ML/I) beam dynamics code**

**Robert Ryne**

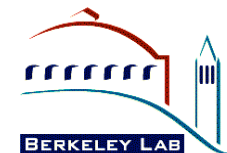
**ComPASS project meeting  
Dec 2, 2008**

MaryLie/IMPACT uses a split-operator approach to combine high-order optics with parallel PIC



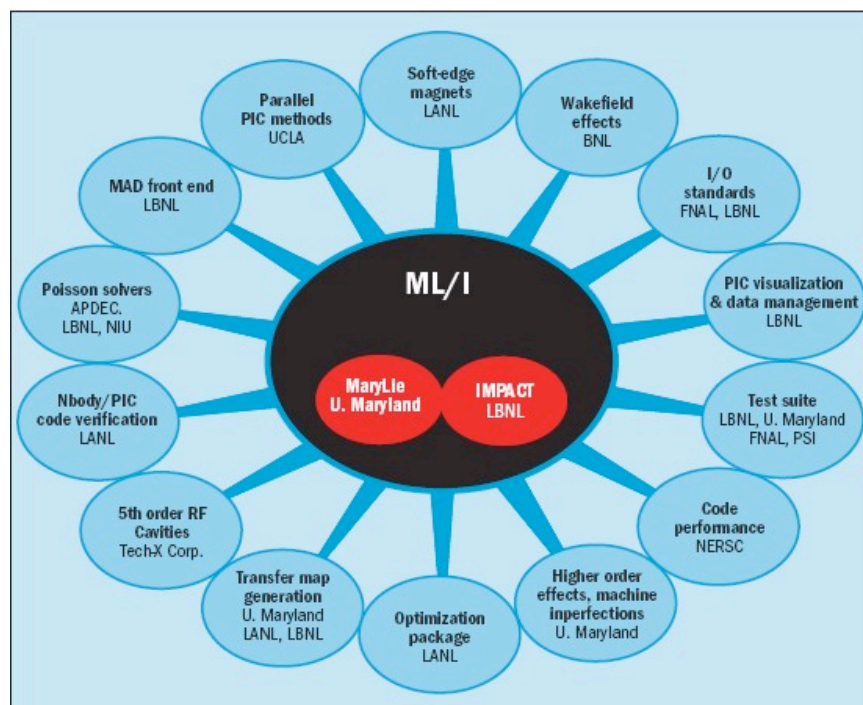
- Note that the rapidly varying s-dependence of external fields is decoupled from slowly varying space charge fields
- Leads to extremely efficient particle advance:
  - **Do not** take tiny steps to push ~100M particles
  - **Do** take tiny steps to compute maps; then push particles w/ maps

# MaryLie/IMPACT (ML/I)



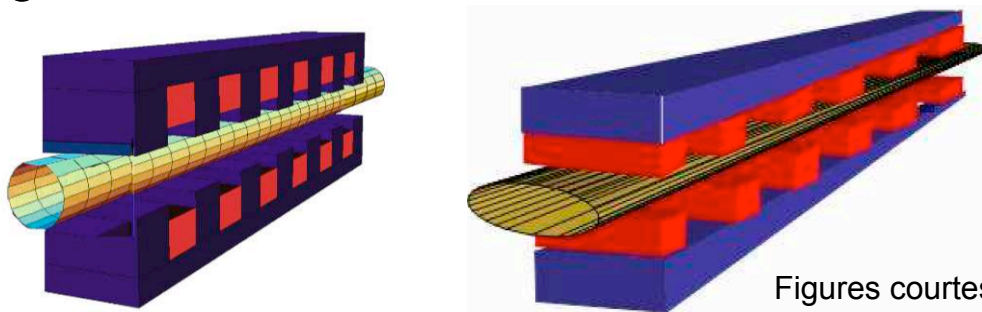
- Combines capabilities of MaryLie code (from U. Md.) with IMPACT code (from LBNL) + new features
- Multiple capabilities in a single unified environment:
  - Map generation
  - Map analysis
  - Particle tracking w/ 3D space charge
  - Envelope tracking
  - Fitting and optimization

- Parallel
- 5th order optics
- 3D space charge
- 5th order rf cavity model
- 3D integrated Green function
- Photoinjector modeling
- Soft-edged magnets
- Coil stacks
- MAD-style input compatibility
- “Automatic” commands
- Test suite



# 5th order RF cavity model

- **Numerical generation of xfer maps for rf cavities described in 1995**
  - R. Ryne, “The linear map for an RF gap including acceleration, LANL Technical Note (1995)
  - R. Ryne, “Finding matched rms envelopes in rf linacs: A Hamiltonian approach,” acc-phys/9502001 (1995).
  - J. van Zeijts, “Arbitrary order transfer maps for RF cavities,” PAC 1995
- **Linear version implemented in IMPACT in 1995 (R. Ryne)**
- **5th order version implemented in MaryLie/IMPACT in 2006 (D. Abell)**
  - D. Abell, Numerical computation of high-order transfer maps for rf cavities, PRST-AB 9, 052001 (2006).
- **Abell paper includes methodology for generation of high order rf cavity generalized gradients from field data**
  - Extends approach previously developed for magnetostatic elements by Dragt, Venturini, Walstrom, and others.



Figures courtesy Alex Dragt, U. Md.

# Integrated Green Function



- Addresses the issue that certain convolution-based Poisson solvers have very poor accuracy when the grid aspect ratio is large
- 2D version w/ linear basis functions described at 2003 ICFA workshop on space-charge simulation, implemented in ML/I
- Independently developed by Ryne (2003), Ohmi (2000), and Ivanov (1989)

## Observations



- The Green function,  $G$ , and source density,  $\rho$ , may change over vastly different scales
- $G$  is known apriori;  $\rho$  is not

We should use all the information available regarding  $G$  so that the numerical solution is only limited by our approximate knowledge of  $\rho$

- Example: 2D Poisson equation in free space

$$\phi(x,y) = \int G(x-x', y-y') \rho(x', y') dx' dy'$$



R. Ryne, ICFA workshop on space-charge simulation, Oxford, April 2-4, 2003



## Standard Approach (Hockney and Eastwood)



$$\phi_{i,j} = \sum G_{i-i', j-j'} \rho_{i',j'}$$

- This approach is equivalent to using the trapezoidal rule (modulo treatment of boundary terms) to approximate the convolution integral
- This approach makes use of only partial knowledge of  $G$
- The error depends on how rapidly the integrand,  $\rho G$ , varies over an elemental volume
  - If  $\rho$  changes slowly we might try to use a large grid spacing; but this can introduce huge errors due to the change in  $G$  over a grid length



R. Ryne, ICFA workshop on space-charge simulation, Oxford, April 2-4, 2003



# Integrated Green Function, cont.



- Assume the charge density,  $\rho$ , varies in a prescribed way in each cell
- Use the analytic form of the Green function to perform the convolution integral exactly in each cell, then sum over cells
- Example: linear basis functions to approximate  $\rho$  in a cell:

$$\begin{aligned}\phi(x_i, y_j) = & \sum_{\tilde{i}, \tilde{j}} \rho_{\tilde{i}, \tilde{j}} \int_0^{h_x} dx' \int_0^{h_y} dy' (h_x - x') (h_y - y') G(x_i - x_{\tilde{i}} - x', y_j - y_{\tilde{j}} - y') + \\ & \sum_{\tilde{i}, \tilde{j}} \rho_{\tilde{i}+1, \tilde{j}} \int_0^{h_x} dx' \int_0^{h_y} dy' x' (h_y - y') G(x_i - x_{\tilde{i}} - x', y_j - y_{\tilde{j}} - y') + \\ & \sum_{\tilde{i}, \tilde{j}} \rho_{\tilde{i}, \tilde{j}+1} \int_0^{h_x} dx' \int_0^{h_y} dy' (h_x - x') y' G(x_i - x_{\tilde{i}} - x', y_j - y_{\tilde{j}} - y') + \\ & \sum_{\tilde{i}, \tilde{j}} \rho_{\tilde{i}+1, \tilde{j}+1} \int_0^{h_x} dx' \int_0^{h_y} dy' x' y' G(x_i - x_{\tilde{i}} - x', y_j - y_{\tilde{j}} - y')\end{aligned}$$

- Shifting the indices results in a single convolution involving an integrated effective Green function:  $\phi_{i,j} = \sum G_{i-\tilde{i}, j-\tilde{j}}^{eff} \rho_{\tilde{i}, \tilde{j}}$



R. Ryne, ICFA workshop on space-charge simulation, Oxford, April 2-4, 2003



# Integrated Green Function: Status in the ComPASS project



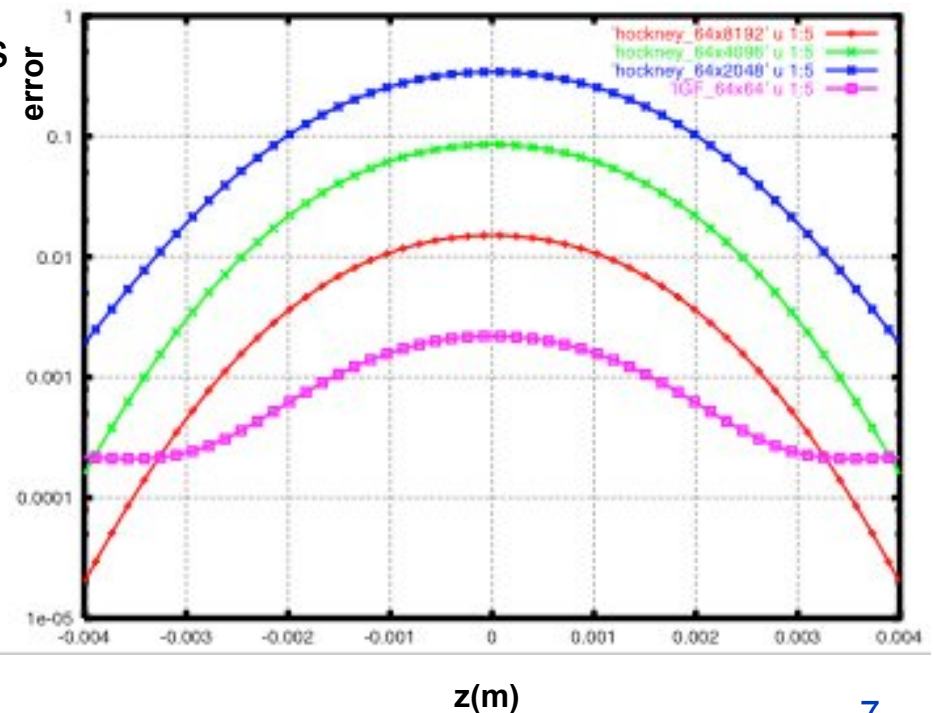
- 3D Version w/ linear basis functions implemented in ML/I (D. Abell)
  - Quad precision version now running on Franklin via D. Bailey's DDFUN package
- 3D Version w/ constant basis functions implemented in IMPACT (J. Qiang)
- 2D Version w/ constant basis functions implemented in BeamBeam3D (J. Qiang)
- Qiang has also invented a shifted IGF for use in computing beam-beam interactions

## References

- D. Abell, "Numerical computation of high-order transfer maps for rf cavities," PRST-AB 9, 052001 (2006).
- J. Qiang, S. Lidia, R. Ryne, C. Limborg-Deprey, "3D quasistatic model for high brightness beam dynamics simulation," Phys. Rev. ST Accel. Beams 9, 044204 (2006). See also Erratum, Phys. Rev. ST Accel. Beams 10, 129901 (2007).
- J. Qiang, M. Furman, R. Ryne, "A parallel particle-in-cell model for beam-beam interaction in high energy ring colliders," J. Comp. Phys. 198, 1, pp. 278-294 (July 2004)
- K. Ohmi, "Simulation of beam-beam effects in a circular  $e^+e^-$  collider," Phys. Rev. E 62, 2000, pp. 7287-7294.
- V. Ivanov, "Numerical methods for analysis of 3D non stationary flows of charged particles," 15 Trudy Instituta Matematiki, Izd-vo "Nauka," Sibirskoe Otdelenie, pp. 172-187 (1989).

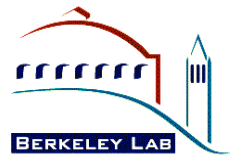
Example: Error in electric field computed using different algorithms applied to a 2D Gaussian elliptical density distribution w/ 500:1 aspect ratio

Hockney: 64x2048, 64x4096, 64x8192  
IGF: 64x64





# ML/I photoinjector capability: Issues



- Z-code or T-code?
  - Z-codes need to convert from “coordinates at fixed z” to “coordinates at fixed t” for each space-charge calc since Poisson is solved at fixed t
  - Z-codes have difficulty w/ space charge unless trajectories are approx linear over a distance equal to the bunch length
    - Could probably use a z-code for a photoinjector, but no one would believe the result unless checked against a t-code. So we’ve implemented a t-code
- Symplectic or Non-symplectic?
  - Symplectic methods essential for studying long-term behavior in circular accelerators. But photoinjector does not involve long-term simulation
    - I don’t expect symplecticity to be essential for photoinjector modeling
    - Other factors might be more important, e.g. adjustable step size for high accuracy near the cathode. So we’ve implemented non-symplectic approach
- Conclusion: use time-based, non-symplectic approach:
  - Numerical simulation of the Lorentz force equations for  $\zeta(t)$  where
$$\zeta = (x, \gamma\beta_x, y, \gamma\beta_y, z, \gamma\beta_z)$$



# Numerical Integration Algorithm



- Integrate particle trajectories using adjustable step Runge-Kutta
  - Pros: easy to implement
  - Cons:
    - uses a lot of memory for temporary vectors (but low storage RK4 might help)
    - Extra space-charge calculations
- Current implementation uses 4th order or 8th order
  - First integrate w/ time step  $h$ ; then integrate w/ two steps of size  $h/2$ 
    - The difference can be used for error control:
      - If difference exceeds  $\varepsilon_1$ , cut step size in half and repeat
      - If difference is below  $\varepsilon_2$ ,
        - » time step is a success
        - » double step size for next step

# RK Error Control



- Straightforward when space charge is absent
  - Base on a single (representative) particle; or maximum over all particles; or average over particles; other choices...
- More complicated when space charge is present
  - Numerical noise in particle-based Poisson solver is problematic
- Current implementation takes a pragmatic approach:
  - Choose a method for error control when space charge is absent
  - Adapt to include space charge; should approach zero-current method as space charge tends to zero
  - When space charge is present, will need to repeat runs with reduced error threshold to verify convergence

**Presently, we use the energy gain of a single particle to determine error associated with a step. We save the space-charge force on this particle at the start of the step and assume it is constant throughout the step. As a result, intra-step space-charge noise is not an issue.**

# Poisson Solver

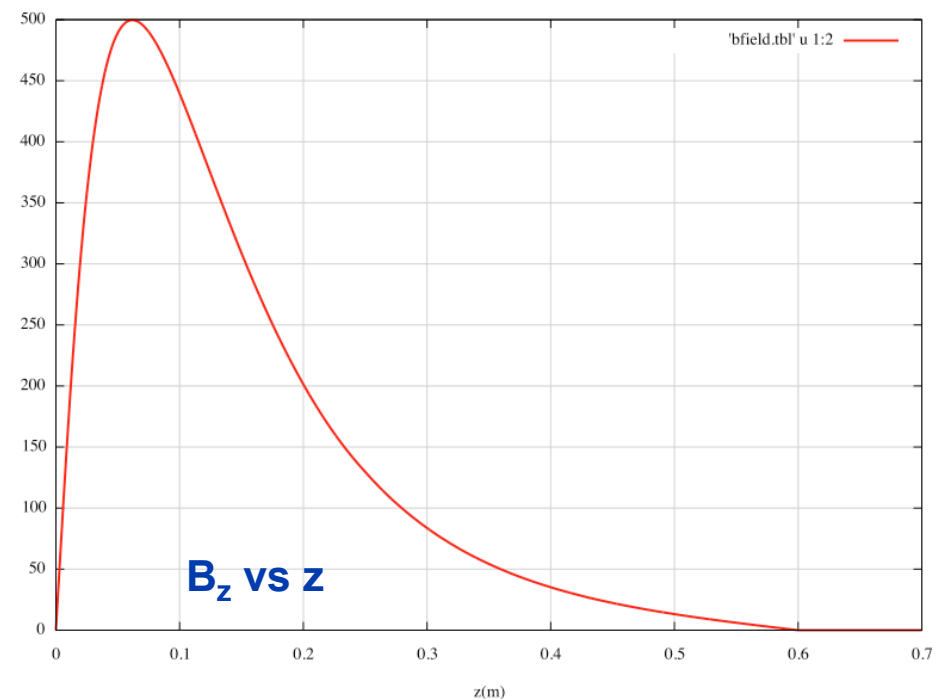
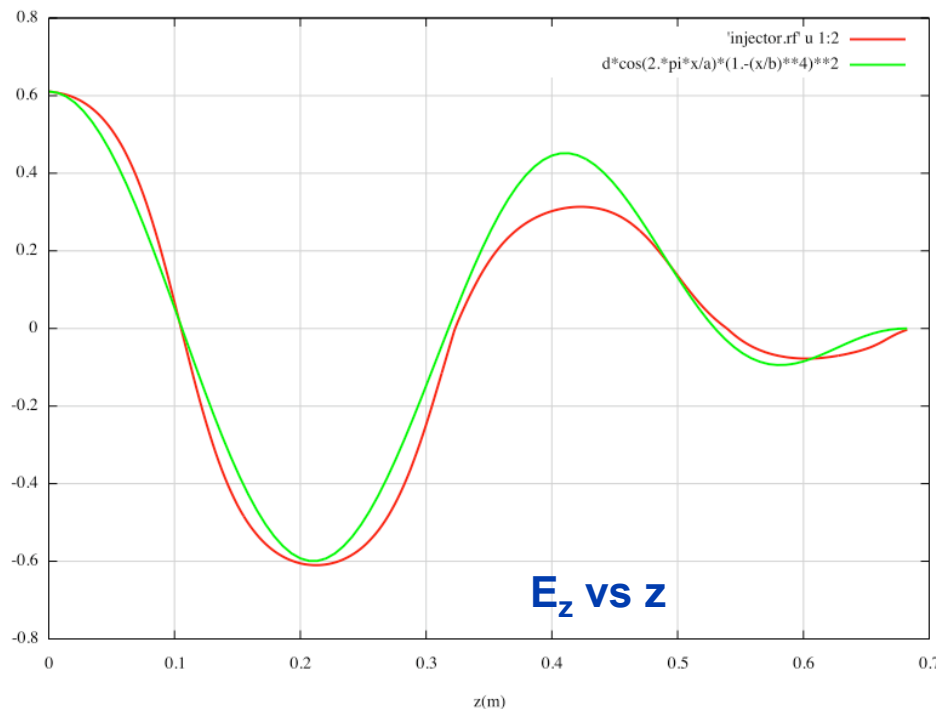


- Use doubled grid convolution (“Hockney algorithm”) to compute space charge subject to open boundary conditions
  - Standard algorithm fails badly due to extreme aspect ratio of the bunch near the cathode
    - Grid cell length  $\sim 100\times$  smaller than transverse cell size
- Use Integrated Green function technique to solve the aspect ratio problem
  - Likely need quad precision if grid aspect ratio  $> 100$
- Image charges of infinite plane cathode included via equal and opposite image charges behind the cathode

# Application

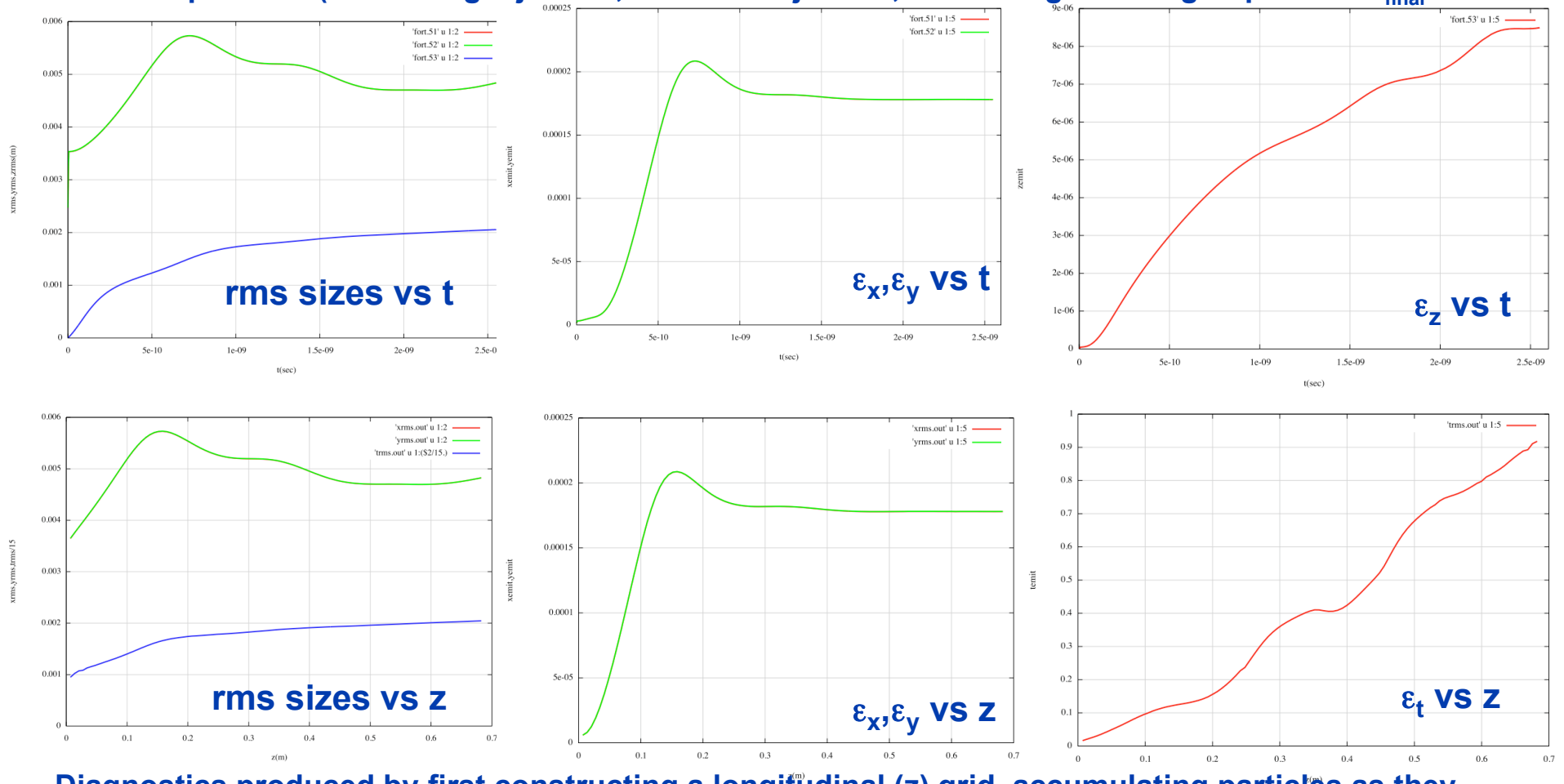


- Test Example:
  - 1 nC, 700 MHz,  $E_{\text{final}}=2.7$  MeV
  - Cathode radius=7 mm,  $E_{\text{emission}}=0-1$  eV,  $\Delta\phi=2.5$  deg
- Simulation parameters: 8M particles, 32x32x512 grid. Error control:
  - if error  $>10^{-10}$ , cut time step ( $\Delta t$ ) in half and repeat step
  - if  $10^{-10} < \text{error} < 10^{-11}$ , step was successful; leave  $\Delta t$  unchanged
  - if error  $< 10^{-11}$ , step was successful; double  $\Delta t$  for next step



# RMS quantities vs t; RMS quantities vs z

Diagnostics vs t produced at each time step of the RK integrator (no extrapolation required). Total # of steps = 533 (100 during injection, 333 after injection, 100 during crossing of plane at  $z_{\text{final}}$ )



Diagnostics produced by first constructing a longitudinal (z) grid, accumulating particles as they advance in time when they cross z-grid points, using 1-step Euler over a fraction of a time step to estimate coordinates at z-crossing point.

# Evolution of energy spread; final phase space



- Gamma values at end of injector:

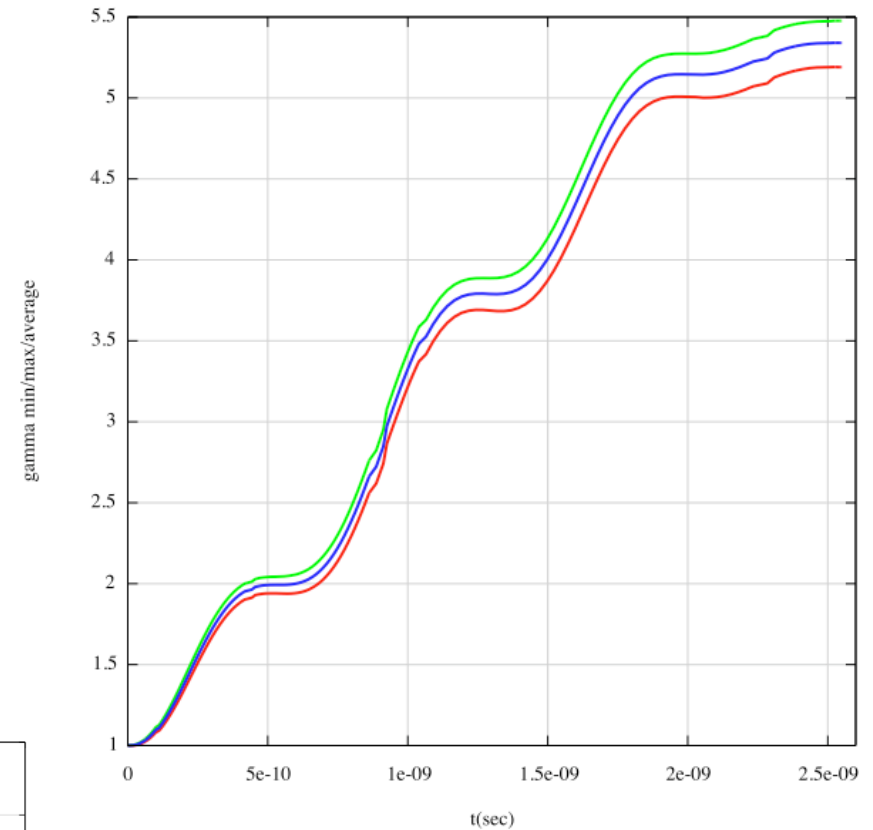
$$\gamma_{\min} = 5.190574164$$

$$\gamma_{\max} = 5.476896407$$

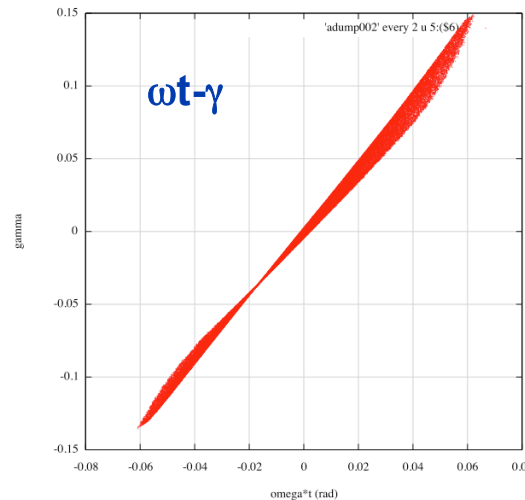
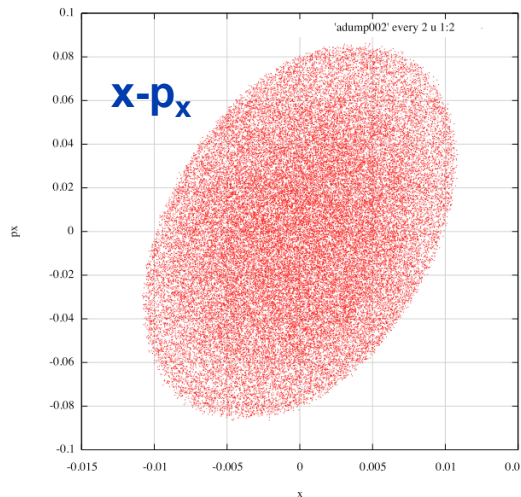
$$\langle \gamma \rangle = 5.340775754$$

$$\langle E_{\text{kin}} \rangle = 2.218107 \text{ MeV}$$

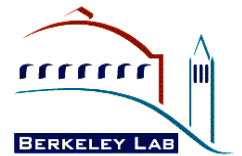
$$\langle E_{\text{tot}} \rangle = 2.729107 \text{ MeV}$$



## Final phase space



# Future Plans



- **Strengthen capability for modeling space-charge in rings**
- **Strengthen capability for modeling ultra-low losses**
- **Complete domain decomposition version of ML/I**
- **Complete development of photoinjector module and distribute to other ComPASS members**
- **Implement new capabilities, as needed, for HEP and NP priorities**